Fusion Engineering and Design 202 (2024) 114331

Contents lists available at ScienceDirect

Fusion Engineering and Design

journal homepage: www.elsevier.com/locate/fusengdes

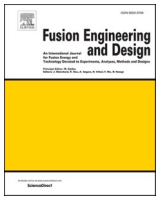

Thermo-mechanical analysis of the components in the launcher transmission line of ITER ex-port plug collective Thomson scattering

Esther Rincón Rincón [a,*], Emilio Blanco [a], Mercedes Medrano [a], Juan José Imaz [b], Yago Villalobos [b], Laura Maldonado [b], Paulo Varela [c], Yong Liu [d], Victor Udintsev [d], Stefan Schmuck [d]

[a] CIEMAT, Fusion National Laboratory, Avda. Complutense 40, 28040 Madrid, Spain
[b] EMPRESARIOS AGRUPADOS, Magallanes 3, 28015 Madrid, Spain
[c] Instituto de Plasmas e Fusão Nuclear, IST, Universidade de Lisboa, 1049-001 Lisboa, Portugal
[d] ITER Organization, Route de Vinon, 13067, St Paul-lez-Durance, France

ARTICLE INFO

Keywords:
ITER
CTS
Diagnostic
Thermo-mechanical analysis
FEM
Miter-bend
Cooling

ABSTRACT

ITER Collective Thomson Scattering (CTS) diagnostic system is designed to analyze the alpha particles resulting from Deuterium-Tritium fusion reactions. It consists of one launcher and nine receiver transmission lines. The launcher line transports the high-power microwave emission of 1.2 MW from the gyrotron source to the front-end, while the receiver lines transport the collected microwave emission from the front-end and distribute it to the instrumentation in the Diagnostic Building.

Due to the high power transported in the launcher line, it has to be water-cooled to minimize the thermal expansion resulting from the heating caused by the power losses. Therefore, this work primarily focuses on establishing the cooling system parameters for the launcher TL to ensure efficient dissipation of the ohmic losses, while meeting the ITER cooling requirements. Once the parameters of the water cooling system are defined, a thermo-mechanical analysis of the most critical components is performed to assess their temperature distribution and deformations.

1. Introduction

The Collective Thomson Scattering (CTS) diagnostic system in ITER is intended to measure plasma parameters related to the projected ion velocity distribution function, in particular of fast ions [1]. The technique used is based on the scattering of a powerful mm-wave beam by the fluctuations in the plasma electron distribution function, which are induced by the fast ions. The radiation scattered in particular directions is collected and measured, providing information about the properties and dynamics of the fast ions [2].

The design of the Ex-Port Plug transmission lines (TL) in ITER is currently in the preliminary stage, with its structural integrity assessment completed [3]. This design consists of one launcher and nine receiver lines, whose layout within the ITER facility is shown in Fig. 1.

The function of the launcher line is to transmit the microwave emission of 1.2 MW, at 60 GHz, from the gyrotron source to the front-end, while the mission of the receiver TLs is to collect the low power scattered radiation and transmit it from the front-end to the instrumentation in the back end.

Due to the high power transported, the transmission line has to be water-cooled to minimize the thermal deformation resulting from the heating caused by the power losses. Therefore, this work will focus first of all on establishing the parameters of the cooling system in the launcher TL that guarantee the dissipation of the ohmic losses while ensuring the compliance with the ITER cooling requirements. Next, a thermo-mechanical analysis of the main components in the launcher TL will be performed to assess their temperature distribution and deformation.

2. Scope

The components under the scope of this work are those of the Ex-Port Plug launcher TL, which is routed from the gyrotron in the Assembly Building 13 (B13), through the Gallery, Port Cell (PC) and Interspace

* Corresponding author.
E-mail address: esther.rincon@ciemat.es (E.R. Rincón).

https://doi.org/10.1016/j.fusengdes.2024.114331
Received 9 October 2023; Received in revised form 9 February 2024; Accepted 7 March 2024
Available online 10 March 2024

(IS) in the Tokamak Building 11 (B11), to the Closure Plate (CP) of the Equatorial Port Plug 12 (EPP12) (see Fig. 1).

The maturity of the design of the components and the cooling water system correspond to the preliminary design stage. Therefore, the results obtained in this work should be taken as a first approach to address the problem, which will be refined throughout the final design process.

3. System description

The components and the cooling system in the CTS launcher TL are similar to those of the ECRH (Electron Cyclotron Resonance Heating) system in ITER, since the gyrotron output power and the TLs are very much alike in both systems. However, the differences in the CTS gyrotron frequency (60 GHz) and the waveguide dimensions (88.9 mm inner diameter) result in distinct power losses, leading to relevant differences in related designs.

As for the Ex-Port Plug launcher line in the CTS, it is about 115 m long, 90 m of which are made of Al 6061-T6 in the current design, with the remaining 25 m made of SS 316 L due to safety and structural reasons. The TL is made up of straight oversized circular corrugated waveguide (WG) segments, with internal diameter of 88.9 mm and maximum length of about 2 m, joined by flanges. The waveguides include four cooling pipes, evenly distributed around the outer surface, which run along the waveguide length as shown in Fig. 2.

In the current design, there are 11 miter bends (MB) installed along the launcher TL to redirect the propagation of the microwave beam, through its reflection at the miter bend mirror. Ten miter bends are at 90°, while the one located in the Gallery next to the PC lintel is at 140° to direct the TL towards EPP12 (see Fig. 1).

Two of the 90° miter bends in the Assembly building are polarizers to allow adjustment of the probing beam polarization. The function of a polarizer MB is like that of a standard one, but the reflector surface is grooved instead of flat. This grated surface makes the power loss to be higher in the polarizer (see Table 1). Since most of the power loss in the launcher TL will be deposited in the miter bends, all of them are made of CuCrZr, with four cooling channels in the mirror to minimize thermal deformation of the mirror surface (see Fig. 3).

The preliminary design of the launcher line also includes expansion units (EU), which are distributed along the line to accommodate differential axial movements of its components, thus avoiding the stresses due to thermal expansion or relative displacements. Although the power loss in the expansion units is very low (see Table 1), they have been made of CuCrZr, with two cooling channels at each side, to avoid the thermal deformation of the sliding surfaces that could otherwise cause the component to seize (see Fig. 4).

Finally, another important component at the end of the launcher line from the cooling point of view is the MOU (Matching Optical Unit),

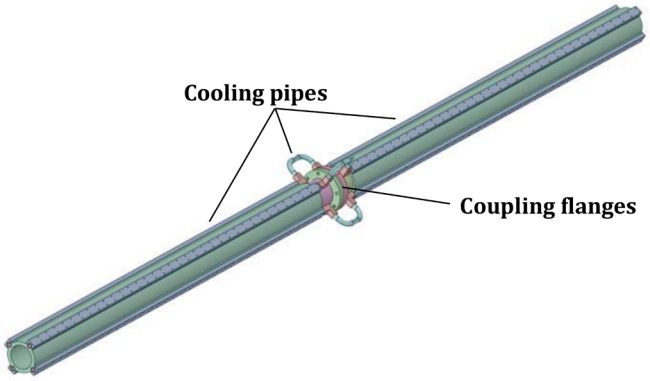

Fig. 2. Waveguides in the launcher TL.

Table 1
Ohmic losses for the components in the scope of this work @ ($f = 60$ GHz, $\varnothing =$ 88.9 mm).

Component	Ohmic Losses per component (kW) (1.2 MW Power Supply)	Quantity	Total Ohmic Losses (kW) (1.2 MW Power Supply)
Al 6061-T6 WG	0.07 kW/m	89.6 m	6.27
SS-316L WG	0.34 kW/m	24.4 m	8.30
90° MB	5.57 kW/MB	8 MB (90°)	44.56
90° MB polarizer	6.72 kW/MB	2 MB (90° Pol.)	13.44
140° MB	11.76 kW/MB	1 MB (140°)	11.76
EU	0.10 kW/EU	11 EU	1.10
TOTAL Losses			**85.43**

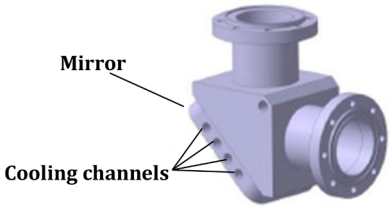

Fig. 3. 90° miter bends in the launcher TL.

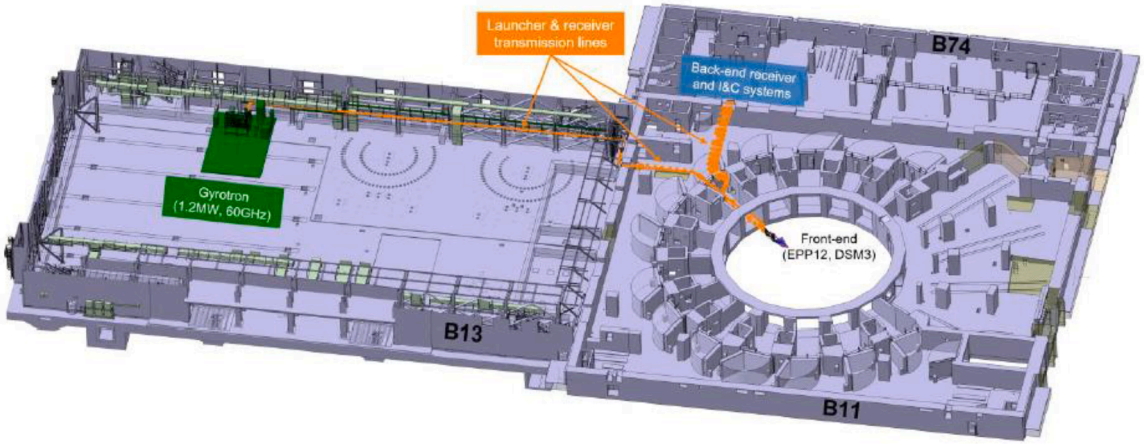

Fig. 1. Layout of the CTS system within the ITER facility (assembly building B13, tokamak hall B11, diagnostic building B74).

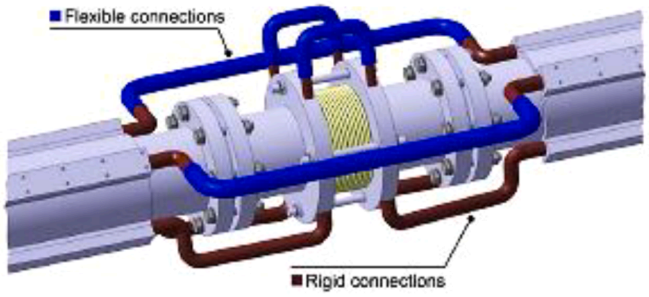

Fig. 4. Expansion unit and cooling arrangement.

which is a multi-mirror arrangement that is connected to the primary window in the CP. During operation, the MOU mirrors will be routing a 1.2 MW beam, so they need to be made of CuCrZr and actively cooled. Since the MOU is cooled independently from the Ex-Port Plug TL cooling circuits [9], it is excluded from this work.

4. Cooling system balance

4.1. Heat losses in CTS components

Ohmic losses in the CTS launcher line are estimated in [4], based on a scaling from the ECH frequency ($f = 170$ GHz) to the CTS frequency ($f =$ 60 GHz) and considering $\varnothing = 88.9$ mm circular corrugated WG [5], taking into account the information available in previous works, namely [6] and [7]. Table 1 applies the ohmic losses estimated in [4] to the components in the scope of this work, for the total power supply of 1.2 MW.

4.2. Connection to ITER component cooling water system (CCWS). Water parameter limits

The CCWS has one loop for the cooling of the tokamak area (CCWS 1A) and another loop for the cooling of the Assembly building (CCWS 2A). Therefore, the cooling circuit of the launcher TL for the IS, PC and Gallery is connected to the CCWS-1A through the connection point shown in Fig. 5. And the cooling circuit of the launcher TL in the Assembly Building is connected to the CCWS 2A, through the connection point shown in Fig. 6.

The limiting values for the parameters of the cooling water (CW) supplied by CCWS-1A and CCWS-2A loops are summarized in Table 2.

4.3. Cooling system calculation. Methodology

A sensitivity analysis is performed for the total power and total flow, in an iterative process similar to that followed in [8], until all input/output parameters comply with the limits imposed in Table 2. The iterative process consists of the following steps:

1. Mass flow rate ($\dot{m}$) values are set for every loop.

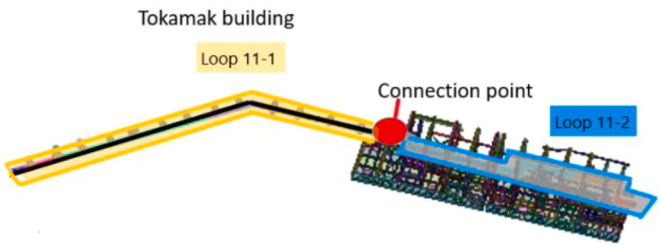

Fig. 5. Connection point to CCWS-1A in the tokamak building.

2. The temperature increments (ΔT) associated with the water mass flow rates ($\dot{m}$), to remove the thermal power ($\dot{Q}$), are calculated according to the following expression (1), in which c_p is the specific heat of water (J/(kg K)).

$$\Delta T = \dot{Q}/(\dot{m}c_p) \tag{1}$$

3. The velocity of the cooling water is calculated, considering different standard diameters of the cooling channels, according to the following expression (2), in which v is the water flow velocity (m/s), Q is the volumetric flow rate (m^3/s) and S is the cooling channel section (m^2).

$$v = Q/S \tag{2}$$

The velocity for cooling systems is recommended to be lower than 3.6 m/s. Therefore, diameters leading to velocities higher than 3.6 m/s are discarded.

4. The pressure drop (ΔP) is calculated with the program *SF Pressure drop*. A cross-check is performed applying the expression (3) for straight pipes, in which ρ is the water density (kg/m^3), L and D are the length and inner diameter of the cooling channels (m). *f(Re, e/D)* is the friction factor, which can be calculated through the Moody diagram, based on the relative roughness (e/D), assuming that the roughness (e) for the Cu cooling channels is 0.003 mm, and the Reynolds number (Re) defined in the expression (4), in which μ is the dynamic viscosity of the water (kg/(m s)).

$$\Delta P = f\rho V^2 L/2D \tag{3}$$

$$\mathrm{Re} = \rho VD/\mu \tag{4}$$

Additional 20 % in length is considered in L to take into account the bend connections.

5. If the values obtained for the water parameters do not meet the limits defined in Table 2, then the inlet flow in the connection to the CCWS-1A and/or CCWS-2A is split in different loops, repeating the process (steps 1 to 5) for every loop until they comply with the limits.

4.4. Cooling system calculation. Results

After several iterations, the conclusion is that the cooling for the launcher line has to be separated into different cooling loops in order to keep the return temperature, velocity and pressure drop under the limits, respecting the maximum overall flowrate available (Fig. 7).

As a result, the inlet flow in the connection to the CCWS-1A has been split in two different loops for the cooling of the launcher TL in B11: loop 11-1 for the TL in the PC and Gallery; and loop 11-2 for the TL in the Port Cell Support Structure (PCSS) and Interspace Support Structure (ISS) (see Fig. 5). On the other hand, the inlet flow in the connection to the CCWS-2A has been split in two different loops (loop 13-1 and loop 13-2) for the cooling of the launcher TL in the Assembly building (see Fig. 6).

The mass flow rate of 0.7 kg/s in every loop keeps the pressure drop well within the limits for CCWS-1A and CCWS-2A, with acceptable values of the water flow velocity for the standard inner diameter of 16 mm, which is compatible with the preliminary design of the components in the launcher TL. The resulting parameters in every loop are summarized in Tables 3 and 4.

5. Thermo-mechanical analysis

A steady state thermal analysis is performed in Ansys Workbench for the most significant components in the launcher TL in order to check the temperature distribution, followed by a static structural analysis to evaluate the expected thermal deformations. These analyses are based in

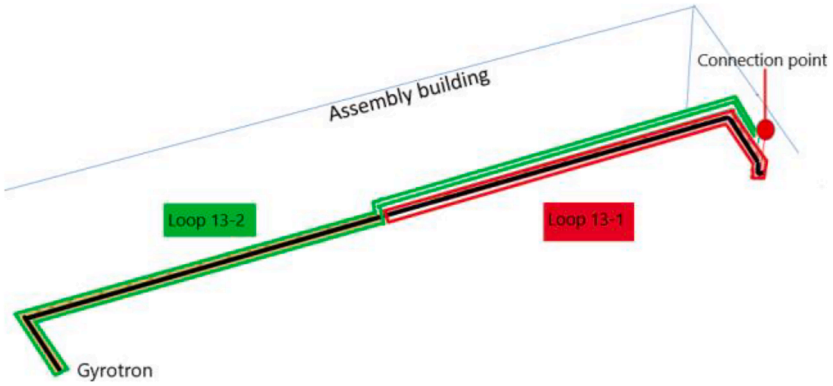

Fig. 6. Connection point to CCWS-2A in the assembly building.

Table 2
Parameters of the CW supplied for the cooling of the launcher line in the Tokamak and Assembly buildings.

Parameter	CTS CW Tokamak building (CCWS-1A)	CTS CW Assembly building (CCWS-2A)
CW supply temperature, Ts (max/min, °C)	34/28	31/25
CW return temperature CTS, Tr (max, °C)	48	39
CW supply/return temperature increment, ΔT (max, °C)	14	8
CW supply pressure, Ps (max, MPa)	1.0	0.8
Pressure drop of CW within CTS cooling system, ΔP (max @ nominal flow, MPa)	0.4	0.4
CW mass flow rate, $\dot{m}$ (nominal, kg/s)	1.7	4.2

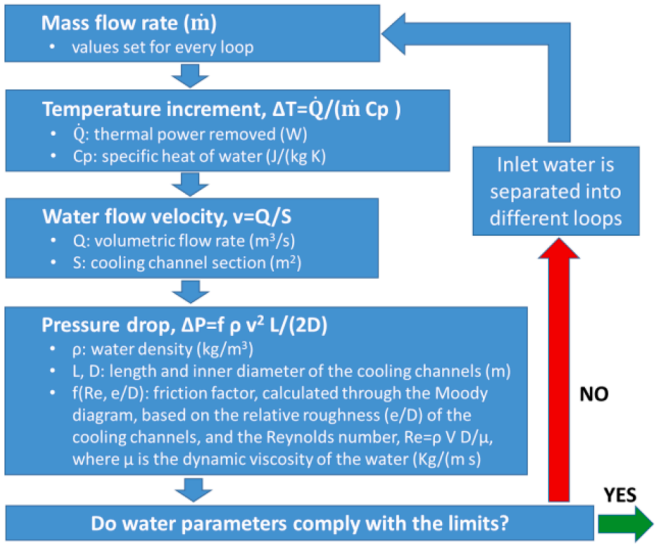

Fig. 7. Iterative process followed for the cooling system calculation.

the previous ones performed in the ECRH System [10,11,12].

Individual finite element models (FEM) are developed for every component, considering the worst case in terms of material, applied loads and boundary conditions. The components included in these models are listed below:

Table 3
Components and CW parameters in the Tokamak Building 11 cooling loops.

Components and parameters	Loop 11-1 (PC & Gallery)	Loop 11-2 (PCSS & ISS)
Components	9.3 m WG (Al) 10 m WG (SS) 1 MB (140°) 2 EU	14.4 m WG (SS) 6 MB (90°) 5 EU
Power losses (kW)	16.01	38.82
CW Mass flow rate, $\dot{m}$ (kg/s)	0.7	0.7
CW temperature increment, ΔT (°C)	5.5	13.2
Cooling channel inner diameter, D (mm)	16	16
CW Pressure drop, ΔP (MPa)	0.10	0.13

Table 4
Components and CW parameters in the Assembly Building 13 cooling loops.

Components and parameters	Loop 13-1 (close to the connection point)	Loop 13-2 (close to the Gyrotron)
Components	40 m WG (Al) 1 MB (90°) 2 MB (9° Pol.) 2 EU	40.3 m WG (Al) 1 MB (90°) 2 EU
Power losses (kW)	22.01	8.59
CW Mass flow rate, $\dot{m}$ (kg/s)	0.7	0.7
CW temperature increment, ΔT (°C)	6.8	3.0
Cooling channel inner diameter, D (mm)	16	16
CW Pressure drop, ΔP (MPa)	0.16	0.26

- FEM-1: Two SS316L waveguide segments joined with a flange (see Fig. 2).
- FEM-2: Two SS316L waveguide segments joined with a CuCrZr Expansion Unit (see Fig. 4).
- FEM-3: One CuCrZr 90° Polarizer miter bend (see Fig. 3).

The mesh in the FEM is made of Ansys Solid-87 and Solid-90 elements.

Boundary conditions for thermal and mechanical analyses are defined in Section 5.1, and applied loads in Section 5.2.

5.1. Boundary conditions

Boundary conditions for the steady-state thermal analysis are defined by the convection in the cooling channels (Section 5.1.1) and in the outer surface of the component (Section 5.1.2). In the static

structural analysis, boundary conditions are defined by restricting the degrees of freedom necessary to fix the component isostatically (Section 5.1.3).

5.1.1. Convection in the inner surface of the cooling channels

Convection in the inner surface of the cooling channels is defined by the heat transfer coefficient h (W/(m^2 K)), which is obtained through the Reynolds (Re), Prandt (Pr) and Nusselt (N_{UD}) numbers, according to the following expressions:

$$Re = 49179, \text{as per expression} \tag{5}$$

$$Pr = \mu c_p / K = 3.71 \tag{6}$$

$$N_{UD} = 0.0395 Re^{0.75} Pr^{1/3} = 201.9 \tag{7}$$

$$h = N_{UD} K / D = 8051\ \mathrm{W}/\left(\mathrm{m}^2\ \mathrm{K}\right) \tag{8}$$

The cooling water is considered to be at the maximum temperature of 48 °C, as a conservative assumption.

5.1.2. Convection in the outer surface of the component

Regarding the heat flow in the outer surface, there are two situations, depending on the safety classification of the components:

- Safety Important Class (SIC) components are fire protected, so conservatively perfect insulation should be considered in the outer surface.
- Non-SIC components in the Assembly building do not have passive fire protection (PFP), so heat flow to ambient air should be considered in the outer surface.

To evaluate the worst case scenario, all components in the analyses are considered as fire protected. Therefore, Heat Flow = 0 W is considered in the outer surface.

5.1.3. Degrees of freedom fixed

For the models FEM-1 and FEM-2, including two WG segments assembled with the flange and with the EU, all six degrees of freedom have been fixed in the center of gravity of the model.

However, in the MB model (FEM-3) it is the center of the mirror that is fixed in the six degrees of freedom, since the objective of the analysis is to evaluate the deformation of the mirror surface.

5.2. Thermal loads applied

When estimating the thermal loads to be applied in each FEM, it has to be considered that the heat deposited on the MB mirror is only a fraction of the total heat on the MB reported in Table 1. The remaining ohmic losses that are not heating the mirror heat the adjacent waveguides, up to an approximate distance of 15 m in both directions. In consequence, in order to evaluate the worst case scenario, the WGs in FEM-1 and FEM-2 will be assumed to be close to a MB, so the losses coming from the MB will have to be added to those on the WG reported in Table 1. Taking this into account, Table 5 shows the heat loads applied to each.

Table 5
Thermal loads applied to FEMs.

Model	Individual heat load	Total heat load applied
FEM-1 2 WG	In WG: 0.34 kW/m From MB: 0.15 kW/m	In WG: 0.49 kW/m
FEM-2 2 WG+EU	In WG: 0.34 kW/m From MB: 0.15 kW/m In EU: 0.10 kW	In WG: 0.49 kW/m In EU: 0.10 kW
FEM-3 Polarized MB 90°	On MB mirror: 2.32 kW	On mirror reflective area: 2.32 kW

The heat load in FEM-1 (0.49 kW/m) is equivalent to a heat flux of 1729 W/m^2 applied on the inner surface of the waveguides.

The same heat flux will be applied on the inner surfaces of the WGs in FEM-2, with an additional heat load of 0.10 kW concentrated in the inner area of the fully closed expansion unit.

As per the heat loads of 2.32 kW in FEM-3, they are concentrated in the ellipse of the mirror reflective area, according to the Gaussian distribution given in the expression (8) for polarized MB at 90°:

$$\dot{q}(x,y) = 981863.45\exp\left(-\left(\left(x^2 + y^2/2\right)/0.0231^2\right)\right) \tag{9}$$

Where $\dot{q}$ is the heat load per surface unit (W/m^2) and (x, y) are the coordinates in a Cartesian reference system in the direction of the minor and major axis of the ellipse and the origin in the center of the mirror reflective area. See Fig. 8 for heat distribution in Polarized MB 90°, according to expression (8).

5.3. Thermal and structural analyses. Results

Temperature results and displacements obtained in the thermal and structural analyses, with the boundary conditions given in Section 5.1 and applied loads in Section 5.2, are summarized in Figs. 9–11:

6. Conclusions

Cooling parameters have been assessed and defined for the preliminary design to meet cooling requirements. These parameters will have to be updated as needed for the final design.

Thermo-mechanical analyses performed in the waveguides show that the maximum temperature is reached in the flanges, where there is no cooling. This temperature (157.6 °C) is far below the maximum admissible for SS316L (about 840 °C). The corresponding axial deformation (<1 mm) is negligible, as well as the maximum radial deformation in the flanges (0.17 mm) when compared to the inner WG radius (44.45 mm). In addition, maximum deformations in the expansion units (26.7 μm) are not expected to compromise the functioning of their sliding surfaces.

Deformations in the MB are focused on the mirror surface, since big deflections could result in unacceptable levels of mode conversion. Deflections obtained (<20 μm) are within the admissible range, but they can be reduced even more in the final design stage with the modification of the cooling channels and the optimization of the cooling parameters.

All the above temperatures should be considered in the final design stage for the detailed analysis of the components.

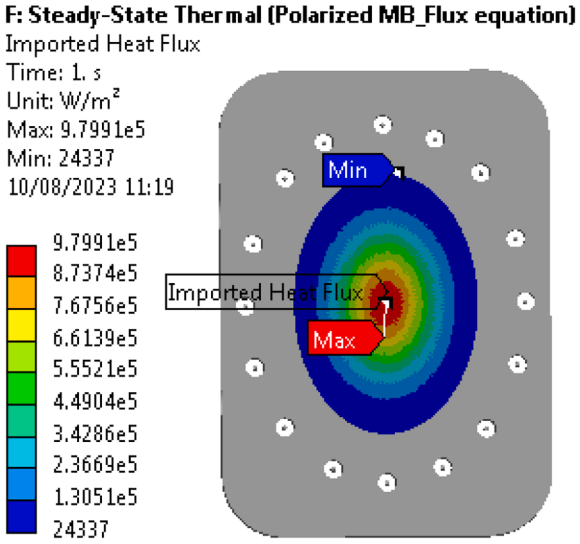

Fig. 8. Heat load applied in Polarized MB 90° as in (8).

Max./Min Temperature	Max./Min deformation
157.6°C / 48.0°C	Axial: 0.98 mm / 0.00 mm
	Max. Radial (flanges): 0.17 mm
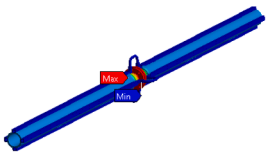	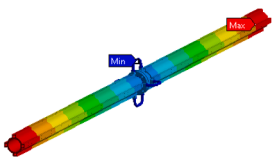

Fig. 9. Temperature and deformation in FEM-1.

Max./Min Temperature	Max./Min deformation
Global: 65.7°C / 48.0°C	Global: 0.57 mm/0.00 mm
EU: 50.1°C / 53.0°C	EU: 26.7 µm /23.5 µm
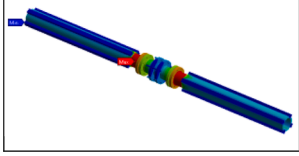	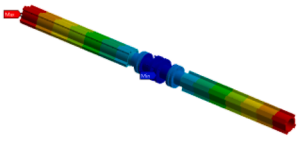

Fig. 10. Temperature and deformation in FEM-2.

Max./Min Temperature in the mirror	Max./Min deformation (normal to reflective area)
105.7°C /51.1°C	19.8 µm/0.00 µm
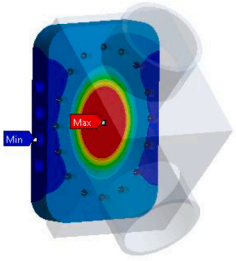	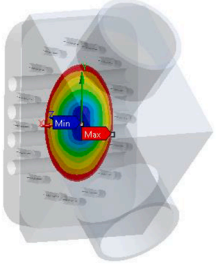

Fig. 11. Temperature and deformation in FEM-3.

Disclaimer

The work leading to this publication has been partially funded by ITER Organization under Implementing Agreement No. 1 (ITER ref. IO/20/CT/4300002249). The views and opinions expressed herein do not necessarily reflect those of the ITER Organization.

CRediT authorship contribution statement

Esther Rincón Rincón: Conceptualization, Data curation, Formal analysis, Investigation, Visualization, Writing – original draft, Writing – review & editing. **Emilio Blanco:** Conceptualization, Investigation, Methodology, Validation. **Mercedes Medrano:** Project administration, Resources, Supervision. **Juan José Imaz:** Formal analysis, Investigation, Methodology, Software. **Yago Villalobos:** Formal analysis, Investigation. **Laura Maldonado:** Formal analysis, Investigation. **Paulo Varela:** Investigation, Validation. **Yong Liu:** Funding acquisition, Project administration, Validation. **Victor Udintsev:** Funding acquisition, Project administration, Validation. **Stefan Schmuck:** Funding acquisition, Project administration, Validation.

Declaration of competing interest

The authors declare that they have no known competing financial interests or personal relationships that could have appeared to influence the work reported in this paper.

Data availability

The authors do not have permission to share data.

References

[1] S.B. Korsholm, et al., ITER collective Thomson scattering-preparing to diagnose fusion-born alpha particles, Rev. Sci. Instrum. 93 (10) (2022), https://doi.org/10.1063/5.0101867.
[2] H. Bindslev, et al., Fast ion collective Thomson scattering, JET results and TEXTOR plans, Fusion Eng. Des. 53 (1–4) (2001) 105–111, https://doi.org/10.1016/S0920-3796(00)00483-X.
[3] E. Rincón, et al., Structural Analysis of the ex-port plug collective Thomson scattering transmission lines for ITER, Fusion Eng. Des. 191 (2023), https://doi.org/10.1016/j.fusengdes.2023.113585.
[4] ITER_D_7HCQM5 v1.0 - 55.C7.C0/D0 - Performance Analysis. https://user.iter.org/default.aspx?uid=7HCQM5.
[5] ITER_D_665KPQ v1.0 - ITER_D_665KPQ_TO#02-Del1-IFP Waveguide Loss Estimation v1. https://user.iter.org/?uid=665KPQ.
[6] J.L. Doane, C.P. Moeller, HE11 miter bends and gaps in a circular corrugated waveguide, Int. J. Electron. 77 (4) (1994) 489–509, https://doi.org/10.1080/00207219408926081.
[7] J.L. Doane, Propagation and mode coupling in corrugated and smooth- wall circular waveguides, in: K.J. Button (Ed.), Infrared and Millimeter Waves 13, Academic Press, Inc., 1985, pp. 123–170. Ch. 5.
[8] M. Parro, et al., Design and analysis of the IFMIF–EVEDA beam dump cooling system, Fusion Eng (2012), https://doi.org/10.1016/j.fusengdes.2012.02.018.
[9] H. Policarpo, et al., Conceptual design of cooling systems for the launcher and receiver mirrors of the ITER LFS-CTS diagnostic, Fusion Eng. Des. 131 (2018) 61–76, https://doi.org/10.1016/j.fusengdes.2018.04.067.
[10] A. Allio, et al., Assessment of the performance of different cooling configurations for the launcher mirrors of the ECRH system of the DTT facility, IEEE Trans. Plasma Sci. 50 (11) (2022) 4054–4059, https://doi.org/10.1109/TPS.2022.3182532.
[11] P.S. Silva, et al., Design concept and thermal-structural analysis of a high power reflective mm-wave optical mirror (M2) for the ITER ECH-UL, Fusion Eng. Des. 146-A (2019) 618–621, https://doi.org/10.1016/j.fusengdes.2019.01.037.
[12] D. Li, et al., Preliminary design and thermo-mechanical analysis of the ECRH equatorial launcher focusing mirror (M1) towards the CFETR, Fusion Eng. Des. 191 (2023) 113723, https://doi.org/10.1016/j.fusengdes.2023.113723.